Stereoelectronic effects in a homologous series of bidentate cyclic phosphines. A clear correlation of hydroformylation catalyst activity with ring size†

Mairi F. Haddow,[a] Ann J. Middleton,[a] A. Guy Orpen,[a] Paul G. Pringle*[a] and Rainer Papp[b]

Received 29th August 2008, Accepted 14th October 2008
First published as an Advance Article on the web 25th November 2008
DOI: 10.1039/b815056g

The homologous series of diphosphines $(CH_2)_{n-1}P(CH_2)_3P(CH_2)_{n-1}$ where $n = 5$ ($\mathbf{L_5}$), 6 ($\mathbf{L_6}$), or 7 ($\mathbf{L_7}$) have been synthesized from the corresponding $PhP(CH_2)_{n-1}$. Treatment of $[PtCl_2(cod)]$ with $\mathbf{L_{5-7}}$ gave the 6-membered chelates *cis*-$[PtCl_2(\mathbf{L_{5-7}})]$, the crystal structures for which reveal that $\mathbf{L_{5-7}}$ have very similar steric bulk and bite angles. Treatment of $[Rh_2Cl_2(CO)_4]$ with $\mathbf{L_{5-7}}$ gave the binuclear *trans*-$[Rh_2Cl_2(CO)_2(\mu\text{-}\mathbf{L_{5-7}})_2]$ with *syn* and *anti* orientations of the CO and Cl ligands suggested by the ^{31}P NMR spectra and the crystal structures of *syn–trans*-$[Rh_2Cl_2(CO)_2(\mu\text{-}\mathbf{L_5})_2]$ and *anti–trans*-$[Rh_2Cl_2(CO)_2(\mu\text{-}\mathbf{L_7})_2]$. The ν(CO) values for *trans*-$[Rh_2Cl_2(CO)_2(\mu\text{-}\mathbf{L_{5-7}})_2]$ indicate that the donor strength increases in the order $\mathbf{L_5} < \mathbf{L_6} < \mathbf{L_7}$. A study of rhodium-catalysed hydroformylation of 1-octene using diphosphines $\mathbf{L_{5-7}}$ is described. The catalyst activity decreases with increasing phosphacycle ring size: $\mathbf{L_5} > \mathbf{L_6} > \mathbf{L_7}$.

Introduction

Monodentate and bidentate phosphacycles of a variety of types and sizes are excellent ligands for hydroformylation catalysis as illustrated by the examples $\mathbf{L_{A-H}}$ given in Fig. 1.

Phosphacyclic ligands often give more active, selective and stable catalysts than their linear analogues. Delineating factors that influence the efficiency of catalysts for hydroformylation is apparently easy, understanding them remains a challenge.[1,2] In the case of phosphacycles, the features that lead to their advantages include: (i) the entropic stabilisation of the P–X bonds in phosphacycles, (ii) the conformational rigidity of the ring and (iii) the constraints on the X–P–X angle imposed by the ring. Thus, the kinetic stabilisation of the P–O bonds in cyclic phosphites,[3] such as $\mathbf{L_A}$ or the P–N bonds in cyclic phosphamides,[4] such as $\mathbf{L_B}$ make them less susceptible to hydrolysis than acyclic analogues and this has greatly contributed to their utility. The rigidity of ligands such as $\mathbf{L_C}$,[5] $\mathbf{L_D}$[6] and $\mathbf{L_E}$,[7] make the α-substituents sterically demanding, which may contribute to the high hydroformylation catalytic activity of their rhodium complexes. The ring rigidity in $\mathbf{L_F}$ results in a highly defined chiral space around the metal centre, which may account for the success of $\mathbf{L_F}$ and related ligands in asymmetric hydroformylation.[8] The constrained C–P–C angle imposed by the phosphacycle influences the frontier orbital energies[9] thereby modulating the σ-donor and π-acceptor characteristics of the ligand and this may partly explain the high activity of hydroformylation catalysts derived from phosphacycles such as $\mathbf{L_G}$[10] and $\mathbf{L_H}$.[11]

As is evident from the examples in Fig. 1, phosphacycles with ring sizes from 5–7 are important for hydroformylation catalysis. We are interested in understanding the effect the size of the ring has on the coordination chemistry and catalytic performance of P-ligands.[7,12,13] Recently, we reported a systematic study of the homologous series of cyclic monophosphines **1a–c** and their application in rhodium-catalysed hydroformylation.[12] From spectroscopic measurements, it was found that the donor order was **1a** < **1b** < **1c**, which is in line with the prediction that the more acute the C–P–C angle is made, the lower the HOMO and LUMO energies on the ligand become.[9] The steric properties of the monophosphacycles (particularly **1c**) were shown to depend

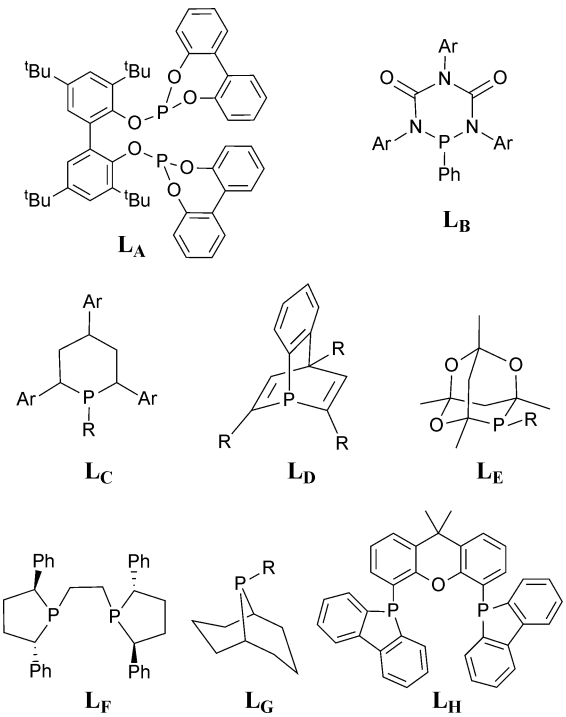

$\mathbf{L_A}$ $\mathbf{L_B}$ $\mathbf{L_C}$ $\mathbf{L_D}$ $\mathbf{L_E}$ $\mathbf{L_F}$ $\mathbf{L_G}$ $\mathbf{L_H}$

Fig. 1 Examples of phosphacyclic ligands used in hydroformylation catalysis.

[a]*School of Chemistry, University of Bristol, Cantocks Close, Bristol, UK BS8 1TS. E-mail: paul.pringle@bristol.ac.uk; Fax: +44 (0)117 929 0509; Tel: +44 (0)117 928 8114*
[b]*BASF Aktiengesellschaft, D-67056 Ludwigshafen, Germany*

† CCDC reference numbers 700268–700272. For crystallographic data in CIF or other electronic format see DOI: 10.1039/b815056g

critically on the ring conformation but no clear trend emerged from the hydroformylation catalysis study with **1a–c** and related ligands.[12] Part of the problem with discerning structure–activity relationships with monodentate ligands is the variable number (between 0 and 3) of ligands that may be coordinated to the metal and the *cis*/*trans*/axial/equatorial geometric relationships to each other that they adopt in the catalytic intermediates. We reasoned that the number of variables would be reduced, and therefore clearer trends may emerge, using the cyclic diphosphines $\mathbf{L}_{5-7}$.

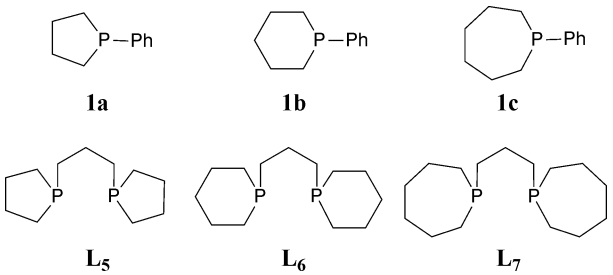

Results and discussion

Ligand synthesis

The series of bidentate cyclic phosphines $\mathbf{L}_{5-7}$ were synthesised by the route shown in Scheme 1. The phosphacycles[12] **1a–c** were quaternized with 1,3-dibromopropane to give the corresponding phosphonium salts **2a–c** as air-stable solids. Refluxing these salts in aqueous sodium hydroxide[14] yielded the phosphine oxides **3a–c** as white waxy solids. The reduction of **3a–c** with phenylsilane, followed by distillation directly from the hot reaction mixture, produced $\mathbf{L}_{5-7}$. Diphosphines $\mathbf{L}_5$ and $\mathbf{L}_6$ are colourless liquids and $\mathbf{L}_7$ is a low-melting solid (see Experimental for the characterising data); $\mathbf{L}_5$ has been previously reported[15] but $\mathbf{L}_6$ and $\mathbf{L}_7$ are new.

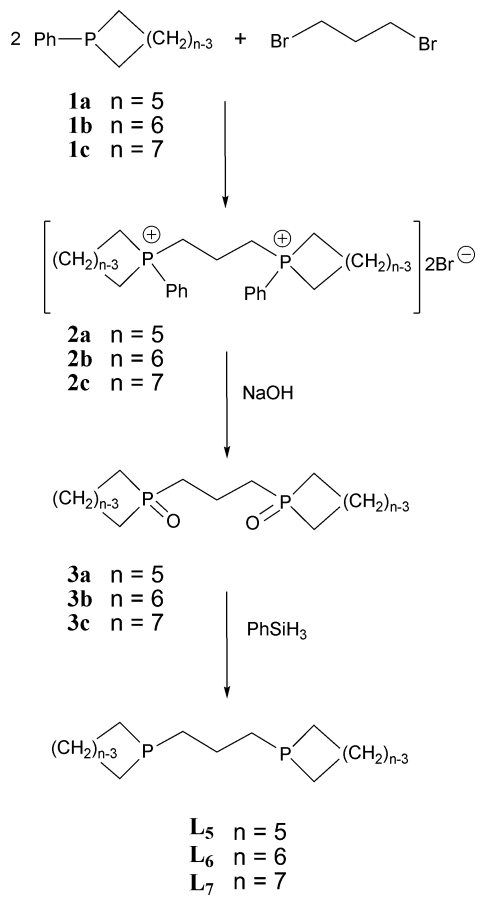

Scheme 1

Platinum(II) complexes

The addition of one equivalent of diphosphines $\mathbf{L}_{5-7}$ to $[PtCl_2(cod)]$ in dichloromethane afforded the corresponding complexes *cis*-$[PtCl_2(\mathbf{L}_{5-7})]$ (**4a–c**) as air-stable, white solids in quantitative yields (eqn (1), see Experimental for the characterising data).

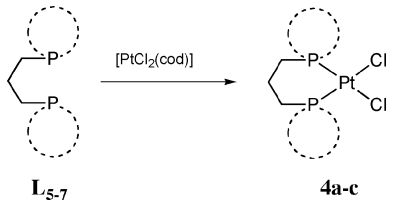

(1)

Crystal structures for all three chelates **4a–c** were obtained (see Fig. 2–4 and Tables 1–3). The chloroform solvate of **4a** crystallises in the space group $P2_12_12_1$ from a saturated $CHCl_3$ solution. The molecule of **4a** (see Fig. 2) has approximate mirror symmetry. Selected bond lengths and angles are given in Table 1.

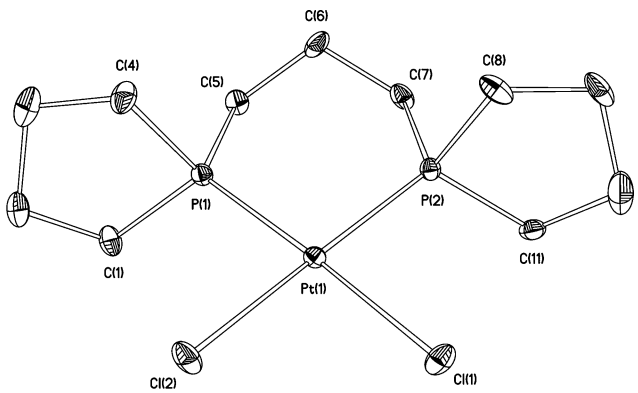

Fig. 2 Thermal ellipsoid plot of the structure of **4a** in **4a**·$CHCl_3$. Displacement ellipsoids are shown at the 50% probability level. All hydrogen atoms have been removed for clarity.

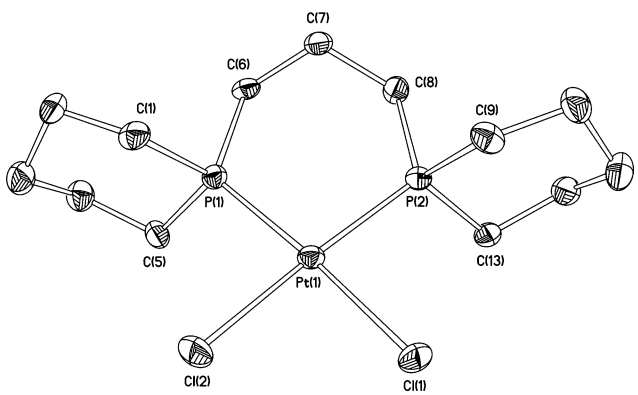

Fig. 3 Thermal ellipsoid plot of the structure of **4b**. Displacement ellipsoids are shown at the 50% probability level. All hydrogen atoms have been removed for clarity.

Table 1 Selected bond distances (Å) and angles (°) for **4a**·$CHCl_3$

Bond distances/Å			
Pt1–P1	2.2143(11)	Pt1–P2	2.2089(11)
Pt1–Cl1	2.3604(10)	Pt1–Cl2	2.3533(10)
P1–C1	1.835(4)	P1–C4	1.828(4)
P1–C5	1.807(4)	P2–C7	1.819(4)
P2–C8	1.822(5)	P2–C11	1.838(4)
Bond angles/°			
P1–Pt1–P2	96.02(3)	C1–P1–C5	104.1(2)
C1–P1–C4	96.26(19)	C4–P1–C5	104.1(2)
C7–P2–C8	104.5(2)	C7–P2–C11	103.5(2)
C8–P2–C11	95.81(19)		

Table 2 Selected bond distances (Å) and angles (°) for **4b**

Bond distances/Å			
Pt1–P1	2.2228(12)	Pt1–P2	2.2289(13)
Pt1–Cl1	2.3716(13)	Pt1–Cl2	2.3774(13)
P1–C1	1.825(5)	P1–C5	1.822(5)
P1–C6	1.823(4)	P2–C8	1.817(5)
P2–C9	1.827(5)	P2–C13	1.827(5)
Bond angles/°			
P1–Pt1–P2	96.48(5)	C8–P2–C9	104.8(2)
C8–P2–C13	104.0(2)	C9–P2–C13	104.0(2)
C1–P1–C5	104.5(2)	C1–P1–C6	104.0(2)
C5–P1–C6	105.6(2)		

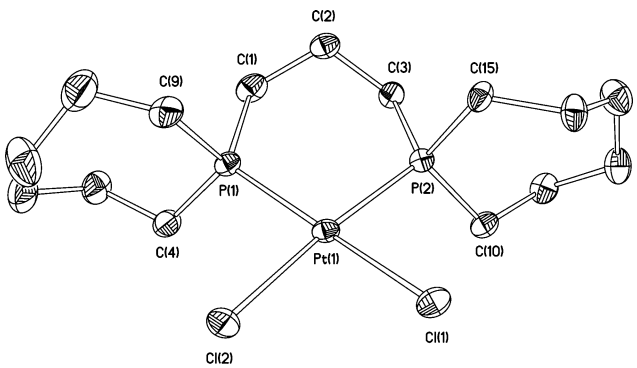

Fig. 4 Thermal ellipsoid plot of the ordered molecule (of three) in the asymmetric unit of the structure of **4c**. Displacement ellipsoids are shown at the 50% probability level. All hydrogen atoms have been removed for clarity.

The five-membered phospholane rings can adopt a range of conformations of which four idealised forms may usefully be identified (Fig. 5). If the phosphorus atom and the two neighbouring carbon atoms are considered to define a reference plane, the other two carbons in the ring can be: (A) in plane with these atoms (planar), (B) one in plane and one out of the plane

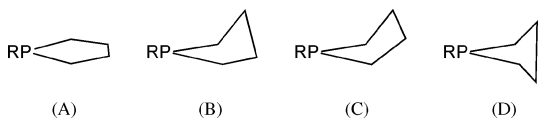

Fig. 5 Conformations of five-membered phospholane rings.

Table 3 Selected bond distances (Å) and angles (°) for **4c**.[a] Parameters for the atoms that were restrained have been omitted

Bond distances/Å					
Pt1–P1	2.2275(17)	Pt2–P3	2.2258(16)	Pt3–P5	2.2303(18)
Pt1–P2	2.2330(15)	Pt2–P4	2.2293(15)	Pt3–P6	2.2347(18)
Pt1–Cl1	2.3719(16)	Pt2–Cl3	2.3740(16)	Pt3–Cl5	2.3636(18)
Pt1–Cl2	2.3884(16)	Pt2–Cl4	2.3898(15)	Pt3–Cl6	2.3921(18)
P1–C1	1.837(6)	P3–C16	1.835(6)	P5–C31	1.811(7)
P1–C4	1.821(6)	P3–C19	1.829(6)		
P1–C9	1.825(6)	P3–C24	1.821(6)		
P2–C3	1.818(6)	P4–C18	1.810(6)	P6–C33	1.814(6)
P2–C10	1.827(6)	P4–C25	1.823(6)	P6–C40	1.823(7)
P2–C15	1.831(6)	P4–C30	1.825(6)	P6–C45	1.827(7)
Bond angles/°					
P1–Pt1–P2	97.09(6)	P3–Pt2–P4	97.00(6)	P5–Pt3–P6	95.24(6)
C1–P1–C4	102.6(3)	C16–P3–C24	102.2(3)		
C1–P1–C9	103.3(3)	C16–P3–C19	103.5(3)		
C4–P1–C9	109.5(3)	C19–P3–C24	110.0(3)		
C3–P2–C10	104.1(3)	C18–P4–C25	103.4(3)	C33–P6–C40	102.6(3)
C3–P2–C15	103.6(3)	C18–P4–C30	103.7(3)	C33–P6–C45	102.2(3)
C10–P2–C15	110.4(3)	C25–P4–C30	110.5(3)	C40–P6–C45	108.6(3)

[a] Equivalent distances for the second and third independent molecules in the asymmetric unit are given in columns 4 and 6. Atoms which are disordered are labelled A or B.

(asymmetric envelope), (C) both above or both below the plane (envelope) or (D) one above and one below the plane (twist). In **4a**, both rings adopt an asymmetric envelope conformation, with the torsion angle C–C–C–C = ± 47.6°.

Crystals of **4b** crystallised from a saturated MeOH solution in the space group *Pbca* with one molecule in the asymmetric unit. Selected bond lengths and angles are given in Table 2. The PC_5 rings adopt a chair conformation with the C_3 chelate backbone and the metal in axial and equatorial sites, respectively (see Fig. 3).

Crystals of **4c** crystallised from a saturated MeCN solution in the space group *Pc* with three molecules in the asymmetric unit. In two of the molecules, significant disorder is present in the PC_6 rings. The molecular geometry (see Table 3) of the only ordered molecule in the crystal structure is shown in Fig. 4. The seven-membered rings in the molecule containing Pt1 adopt twist-chair and boat conformations. In the molecule containing Pt2 they adopt chair conformations with the P atom in a different position in each of the rings and in the molecule containing Pt3 they adopt twist-chair, and chair conformations.[12,16]

From the crystallographic parameters collected in Table 4, it can be deduced that: (1) the intracyclic C–P–C angles increases significantly with increasing ring size, (2) the ligand bite angles increase slightly with increasing ring size and (3) the ligand cone angles (calculated by Tolman's method[17]) show that the ligands have essentially the same bulk.

Table 4 Selected angles (°) from the crystal structures of **4a–c**

Angles/°	**4a**	**4b**	**4c**
Intracyclic C–P–C	96.0[a]	104.3[a]	109.8[b]
P–Pt–P	96.0	96.5	97.0[a]
Tolman cone angle	228	229	225[c]

[a] Average of two. [b] Average of five. [c] Average of three.

Rhodium(I) complexes

Addition of two equivalents of $\mathbf{L}_{5\text{–}7}$ to $[Rh_2Cl_2(CO)_4]$ in CH_2Cl_2 gave two species in each case, which are assigned to the binuclear complexes *trans*-$[Rh_2Cl_2(CO)_2(\mu\text{-}\mathbf{L}_{5\text{–}7})_2]$ as a mixture of *anti*-**5a–c** and *syn*-**5a–c** isomers (eqn (2), see Experimental for characterising data). These structures are assigned on the basis of the ^{31}P NMR spectra, which showed, in each case, two doublets with similar δ(P) and J(RhP) having values typical of a *trans*-$RhCl(CO)(PR_3)_2$ structure.[18] A similar ligand-bridged binuclear structure has been reported for *trans*-$[Rh_2Cl_2(CO)_2(\mu\text{-}Ph_2P(CH_2)_3PPh_2)_2]$.[19]

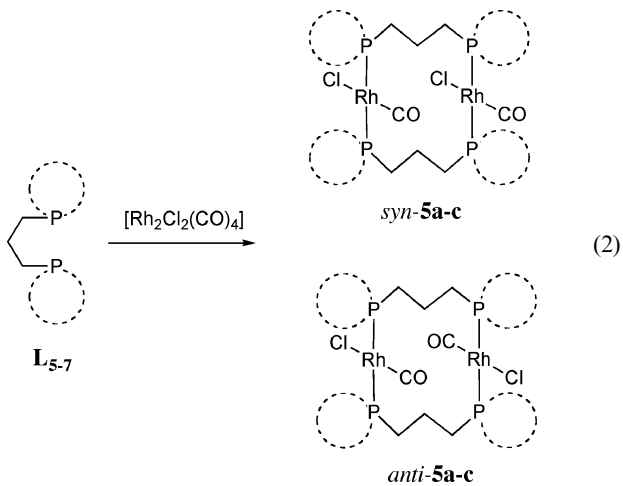

(2)

The crystal structures of *syn*-**5a** and *anti*-**5c** have been determined (see Fig. 6 and 7 and Tables 5 and 6). Crystals of *syn*-**5a** were grown by slow diffusion of diethyl ether into a saturated CH_2Cl_2 solution. The crystals form in the space group $P2_1/c$ with one binuclear molecule in the asymmetric unit. The phospholane rings all adopt distorted asymmetric envelope conformations with four out of five atoms in the ring (including phosphorus) coplanar.

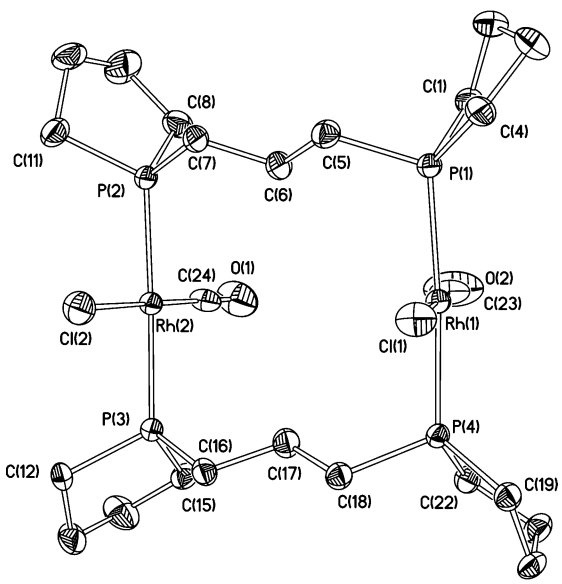

Fig. 6 Thermal ellipsoid plot of the structure of *syn*-**5a**. Displacement ellipsoids are shown at the 50% probability level. All hydrogen atoms have been removed for clarity.

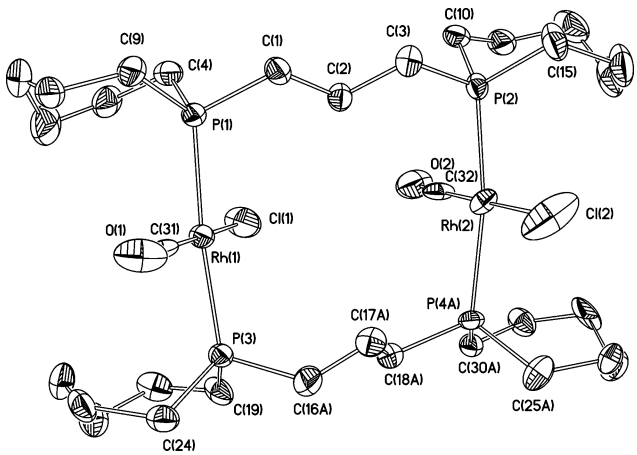

Fig. 7 Thermal ellipsoid plot of the structure of *anti*-**5c**. Displacement ellipsoids are shown at the 50% probability level. All hydrogen atoms have been removed for clarity.

Table 5 Selected bond distances (Å) and angles (°) for *syn*-**5a**

Bond distances/Å			
Rh1–C23	1.805(4)	Rh1–Cl1	2.3714(9)
Rh1–P1	2.3183(9)	Rh1–P4	2.3049(9)
Rh2–C24	1.811(4)	Rh2–Cl2	2.3746(9)
Rh2–P2	2.3017(9)	Rh2–P3	2.3077(9)
P1–C1	1.839(3)	P1–C4	1.852(3)
P1–C5	1.833(4)	P2–C7	1.831(3)
P2–C8	1.839(4)	P2–C11	1.836(4)
P3–C12	1.838(3)	P3–C15	1.847(3)
P3–C16	1.835(3)	P4–C18	1.838(3)
P4–C19	1.836(3)	P4–C22	1.844(3)
Bond angles/°			
C1–P1–C4	94.56(16)	C1–P1–C5	103.68(17)
C4–P1–C5	103.21(17)	C7–P2–C11	104.51(17)
C7–P2–C8	104.57(18)	C8–P2–C11	93.59(18)
C12–P3–C15	94.05(16)	C12–P3–C16	105.84(16)
C15–P3–C16	104.71(17)	C18–P4–C22	103.57(16)
C18–P4–C19	106.55(16)	C19–P4–C22	94.05(16)

The angle between the mean planes of Rh1, P1, P4 and Cl1 and Rh2, P2, P3 and Cl2 is 15.1(1)°. Selected geometric parameters are given in Table 5.

Crystals of *anti*-**5c** were grown by slow diffusion of hexane into a saturated CH_2Cl_2 solution, and form in the space group $P2_12_12_1$ with one binuclear molecule in the asymmetric unit (see, Fig. 7). There is disorder in one of the seven membered rings (involving P4) which was modelled as lying over two conformations in the ratio 0.44 : 0.56. The angle between the mean planes of Rh1, P1, P3 and Cl1 and Rh2, P2, P4 and Cl2 is 41.0(1)°. Selected geometric parameters are given in Table 6.

The IR spectra of **5a–c** showed single absorptions for ν(CO) at 1968 (**5a**), 1963 (**5b**) and 1960 cm^{-1} (**5c**), which are consistent with the donor properties[20] of the ligands being in the order $\mathbf{L}_5 < \mathbf{L}_6 < \mathbf{L}_7$. This is the trend expected[9] on the basis of the crystallographically determined intracyclic C–P–C angles for the phosphines (see below).

Table 6 Selected bond distances (Å) and angles (°) for *anti*-**5c**

Bond distances/Å			
Rh1–C31	1.927(9)	Rh1–Cl1	2.381(2)
Rh1–P1	2.3200(17)	Rh1–P3	2.3160(17)
Rh2–C32	1.807(8)	Rh2–Cl2	2.376(2)
Rh2–P2	2.3111(18)	Rh2–P4A	2.429(10)
Rh2–P4B	2.242(9)		
P1–C1	1.833(6)	P1–C4	1.830(6)
P1–C9	1.833(6)	P2–C3	1.836(5)
P2–C10	1.819(6)	P2–C15	1.822(6)
P3–C16A	1.813(7)	P3–C19	1.837(6)
P3–C24	1.826(6)	P4A–C25A	1.812(18)
P4A–C30A	1.81(3)		

Bond angles/°			
C1–P1–C4	104.4(3)	C1–P1–C9	99.7(3)
C4–P1–C9	101.8(4)	C3–P2–C10	101.8(3)
C3–P2–C15	102.9(3)	C10–P2–C15	101.7(4)
C16A–P3–C19	102.8(3)	C16A–P3–C24	101.2(3)
C19–P3–C24	101.5(3)	C18A–P4A–C25A	106.5(10)
C18A–P4A–C30A	101.7(13)	C25A–P4A–C30A	101.5(19)
C18B–P4B–C25B	104.2(8)	C18B–P4B–C30B	101.9(10)
C25B–P4B–C30B	101.8(14)		

Table 7 Hydroformylation of 1-octene[a]

Entry	Ligand	% Conversion to nonanals	*n* : *iso*
1	$\mathbf{L_5}$	69	2.3
2	$\mathbf{L_6}$	48	2.2
3	$\mathbf{L_7}$	3	2.0

[a] Reactions conditions: 90 °C, 10 bar CO–H_2 (1 : 1) for 4 h in toluene, L–Rh = 5 : 1. See Experimental for details. No decomposition to metallic rhodium was apparent when the autoclaves were opened at the end of a catalytic run. Under more forcing conditions (140 °C, 80 bar), quantitative conversion to aldehyde was observed for all three ligands. No 2-octene was detected in the product of any run and under the same conditions (90 °C, 10 bar, 4 h) the conversions when 2-octene was the substrate were < 1%. The conversions of 1-octene to nonanals are the average of 2 or 3 runs; the differences between individual runs were within 5% for entries 1 and 2 and within 0.5% for entry 3.

Hydroformylation catalysis

Diphosphines with a propane backbone have previously been used in rhodium-catalysed hydroformylation and it is assumed that mononuclear 6-membered chelates are involved in the catalysis.[21] The diphosphines $\mathbf{L_{5-7}}$ were screened for the rhodium-catalysed hydroformylation of 1-octene and the results are given in Table 7. The regioselectivity is similar for the three catalysts which is consistent with the ligands having similar steric bulk.[22] The activity of the catalysts is in the order $\mathbf{L_5} > \mathbf{L_6} > \mathbf{L_7}$, which parallels the order of increasing electronic donation of the three ligands. Thus for this series of isosteric diphosphine ligands containing 5-, 6- or 7-membered phosphacycles, the smaller the ring, the higher the hydroformylation catalytic activity of the derived rhodium complex.

Diphosphine ligands are widely used for hydroformylation and it has been shown that the ligand bite angle and the bulk of the ligand have a significant effect on the efficiency of the catalyst.[1,23] However, the crystal structures of **4a–c** described above show that chelated ligands $\mathbf{L_{5-7}}$ are essentially isosteric and have very similar bite angles. Moreover, the ligand giving the most active catalyst ($\mathbf{L_5}$), has the smallest bite angle while generally, increasing the ligand bite angle above 90° increases the activity of the derived hydroformylation catalysts.[23]

Electronegative substituents on the P-donor often increase the hydroformylation catalytic activity[24] of the Rh complex although this is not always the case.[25] Therefore, we conclude that the phosphacycle ring effect observed here is electronic in origin, confirming the prediction of Orpen and Connelly[9] that reducing the C–P–C angle has the effect of reducing the σ-donor and increasing the π-acceptor properties of the tertiary phosphine.

Experimental

General procedures

Unless otherwise stated, all reactions were carried out under a dry nitrogen atmosphere using standard Schlenk line techniques. Dry N_2-saturated solvents were collected from a Grubbs solvent system[26] in flame and vacuum dried glassware. MeOH was dried over 3 Å molecular sieves and deoxygenated by N_2 saturation. Commercial reagents were used as supplied unless otherwise stated. All phosphines were stored under nitrogen at room temperature. Most complexes were stable to air in the solid state and were stored in air at room temperature. Starting materials $[PtCl_2(cod)]$[27] and $[Rh_2Cl_2(CO)_4]$[28] were prepared by literature methods. Elemental analyses were carried out by the Microanalytical Laboratory of the School of Chemistry, University of Bristol. Electron Impact and Fast Atom Bombardment mass spectra were recorded by the Mass Spectrometry Service, University of Bristol on a MD800 and an Autospec. Infrared spectroscopy was carried out on a Perkin Elmer 1600 Series FTIR. NMR spectra were measured on a Joel GX 300, Jeol Eclipse 400 or Jeol GX 400. $^{31}P\{^1H\}$, $^{13}C\{^1H\}$ and ^1H NMR spectra were recorded at ambient temperature of the probe at 300, 100 and 121 MHz, respectively, using deuterated solvent to provide the field–frequency lock.

Synthesis of 1,3-bis(phenylphospholanium)propane dibromide (2a). 1-Phenylphospholane **1a** (2.11 g, 12.9 mmol) and 1,3-dibromopropane (0.65 cm^3, 1.30 g, 6.45 mmol) in acetonitrile (20 cm^3) were heated at 60 °C for 48 h. The solvent was removed under reduced pressure to give **2a** as a white solid (3.40 g, 6.45 mmol, 100%). Elemental analysis, found (calcd for $C_{23}H_{32}Br_2P_2{\cdot}H_2O$): C 49.85 (50.38), H 6.28 (6.25). ^{31}P NMR (CD_2Cl_2) δ_P/ppm: 49.7 (s). ^1H NMR (CD_2Cl_2) δ_H/ppm: 8.16–8.03 (m, 4H, Ar*H*), 7.74–7.58 (m, 6H, Ar*H*), 3.48–3.23 (m, 8H), 2.60–2.44 (m, 4H), 2.36–1.94 (m, 10H). ^{13}C NMR (CD_2Cl_2) δ_C/ppm: 134.7 (s), 132.6 (m), 130.4 (m), 119.6 (d, ArC_{ipso}, ^1J(PC) 77.6 Hz), 26.9 (m), 23.5 (m), 23.5 (d, PCH_2, ^1J(PC) 51.5 Hz), 17.6 (t, PCH$_2$*C*H$_2$CH$_2$P, ^2J(PC) 2.3 Hz).

1,3-Bis(phenylphosphinanium)propane dibromide (2b). Compound **2b** was made in a similar fashion to **2a** from 1-phenylphosphinane **1b** in 84% yield. Elemental analysis, found (calcd for $C_{25}H_{36}Br_2P_2$): C 53.53 (53.78), H 6.74 (6.50). ^{31}P NMR (CD_2Cl_2) δ_P/ppm: 21.9 (s). ^1H NMR (CD_2Cl_2) δ_H/ppm: 8.20–8.10 (m, 4H, Ar*H*), 7.73–7.66 (m, 2H, Ar*H*), 7.66–7.58 (m, 4H, Ar*H*), 3.21–2.94 (m, 12H), 2.24–2.06 (m, 4H), 2.06–1.90 (m, 2H), 1.87–1.72 (m, 2H), 1.70–1.52 (m, 6H). ^{13}C NMR (CD_2Cl_2) δ_C/ppm: 134.6 (s), 133.1 (m), 130.4 (m), 117.3 (d, ArC_{ipso}, ^1J(PC) 79.2 Hz), 24.9 (m), 24.4 (dd, PCH_2CH$_2$*C*H$_2$P, ^1J(PC) 48.4 Hz,

^3J(PC) 16.1 Hz), 21.4 (m), 18.5 (d, PCH_2, cyclo, ^1J(PC) 47.7 Hz), 16.1 (t, PCH$_2$$CH_2CH_2$P, ^2J(PC) 3.1 Hz).

1,3-Bis(phenylphosphepanium)propane dibromide (2c). Compound **2c** was made in a similar fashion to **2a** from 1-phenylphosphepane **1c** in 90% yield. Elemental analysis, found (calcd for $C_{27}H_{40}Br_2P_2$): C 54.71 (55.31), H 7.24 (6.88). ^{31}P NMR ($CDCl_3$) δ_P/ppm: 33.9 (s). ^{1}H NMR ($CDCl_3$) δ_H/ppm: 8.02–7.92 (m, 4H, Ar*H*), 7.63–7.51 (m, 6H, Ar*H*), 3.27–3.12 (m, 4H), 3.06–2.95 (m, 4H), 2.93–2.79 (m, 4H), 2.17–1.93 (m, 6H), 1.81–1.62 (m, 8H), 1.56–1.41 (m, 4H). ^{13}C NMR ($CDCl_3$) δ_C/ppm: 134.1 (s), 131.9 (m), 130.1 (m), 118.7 (d, ArC_{ipso}, ^1J(PC) 80.0 Hz), 28.7 (s), 25.0 (m), 21.7 (m), 21.4 (d, *J*(PC) 46.9 Hz), 16.4 (m).

Synthesis of 1,3-diphospholanopropane dioxide (3a). To **2a** (3.40 g, 6.45 mmol) was added NaOH (50 cm^3, 20 wt% in distilled water) and the resulting suspension was heated under reflux for 16 h. The product was extracted into $CHCl_3$ (3 × 25 cm^3) and the resulting solution dried over $MgSO_4$. The solvents were removed under reduced pressure to give **3a** as a white solid (1.43 g, 5.76 mmol, 90%). ^{31}P NMR ($CDCl_3$) δ_P/ppm: 70.4 (s). ^{1}H NMR ($CDCl_3$) δ_H/ppm: 2.24–1.66 (m). ^{13}C NMR ($CDCl_3$) δ_C/ppm: 31.5 (dd, P$CH_2$$CH_2$$CH_2$P, ^1J(PC) 60.7 Hz, ^3J(PC) 11.5 Hz), 26.9 (d, PCH_2, cyclo, ^1J(PC) 65.3 Hz), 24.2 (m), 15.7 (t, PCH$_2$$CH_2CH_2$P, ^2J(PC) 3.8 Hz).

1,3-Diphosphinanopropane dioxide (3b). Compound **3b** was made in a similar fashion to **3a** from **2b** in 100% yield. ^{31}P NMR (CD_2Cl_2) δ_P/ppm: 39.0 (s). ^{1}H NMR (CD_2Cl_2) δ_H/ppm: 1.97–1.36 (m). ^{13}C NMR (CD_2Cl_2) δ_C/ppm: 28.9 (dd, P$CH_2$$CH_2$$CH_2$P, ^1J(PC) 64.6 Hz, ^3J(PC) 12.3 Hz), 28.0 (d, PCH_2, cyclo, ^1J(PC) 62.3 Hz), 26.9 (m), 23.1 (m), 14.2 (t, PCH$_2$$CH_2CH_2$P, ^2J(PC) 3.9 Hz).

1,3-Diphosphepanopropane dioxide (3c). Compound **3c** was made in a similar fashion to **3a** from **2c** in 99% yield. ^{31}P NMR ($CDCl_3$) δ_P/ppm: 52.9 (s). ^{1}H NMR ($CDCl_3$) δ_H/ppm: 2.10–1.52 (m). ^{13}C NMR ($CDCl_3$) δ_C/ppm: 31.1 (dd, P$CH_2$$CH_2$$CH_2$P, ^1J(PC) 63.68 Hz, ^3J(PC) 11.5 Hz), 29.8 (s) 29.8 (d, PCH_2, cyclo, ^1J(PC) 62.3 Hz), 21.1 (m), 14.6 (t, PCH$_2$$CH_2CH_2$P, ^2J(PC) 3.9 Hz).

Synthesis of 1,3-diphospholanopropane (L_5). A mixture of **3a** (1.43 g, 5.76 mmol) and phenylsilane (0.98 cm^3, 0.88 g, 8.1 mmol) was heated at 100 °C for 2 h and the evolution of gas was observed. The resulting opalescent viscous liquid was distilled (0.01 mmHg, fraction collected and boiled over the range 100–140 °C) to give $\mathbf{L_5}$ as a clear viscous liquid (0.58 g, 2.69 mmol, 46%). Elemental analysis, found (calcd for $C_{11}H_{22}P_2$): C 60.78 (61.10), H 10.02 (10.25). ^{31}P NMR ($CDCl_3$) δ_P/ppm: –26.7 (s). ^{1}H NMR ($CDCl_3$) δ_H/ppm: 1.89–1.61 (m, 12H), 1.59–1.33 (m, 10H). ^{13}C NMR ($CDCl_3$) δ_C/ppm: 30.4 (dd, P$CH_2$$CH_2$$CH_2$P, ^1J(PC) 16.6 Hz, ^3J(PC) 10.9 Hz), 27.6 (d, *J*(PC) 4.2 Hz), 25.7 (d, PCH_2, cyclo, ^1J(PC) 11.4 Hz), 24.0 (t, PCH$_2$$CH_2CH_2$P, ^2J(PC) 16.6 Hz).

1,3-Diphosphinanopropane (L_6). $\mathbf{L_6}$ was made in a similar fashion to $\mathbf{L_5}$ in 85% yield. b.p. = 112–113 °C, 0.2 mmHg. Elemental analysis, found (calcd for $C_{13}H_{26}P_2$) C 64.38 (63.91), H 11.05 (10.73). ^{31}P NMR ($CDCl_3$) δ_P/ppm: –41.9 (s). ^{1}H NMR ($CDCl_3$) δ_H/ppm: 1.87–1.73 (m, 14H), 1.73–1.62 (m, 4H), 1.58–1.44 (m, 12H), 1.33–1.17 (m, 6H). ^{13}C NMR ($CDCl_3$) δ_C/ppm: 28.7 (dd, P$CH_2$$CH_2$$CH_2$P, ^1J(PC) 13.1 Hz, ^3J(PC) 11.5 Hz), 27.8 (d, *J*(PC) 2.3 Hz), 24.5 (d, PCH_2, cyclo, ^1J(PC) 10.8 Hz), 23.2 (d, *J*(PC) 2.3 Hz), 22.1 (t, PCH$_2$$CH_2CH_2$P, ^2J(PC) 15.4 Hz).

1,3-Diphosphepanopropane (L_7). $\mathbf{L_7}$ was made in a similar fashion to $\mathbf{L_5}$ in 78% yield. b.p. = 117–126 °C, 0.2 mmHg. Elemental analysis, found (calcd for $C_{15}H_{30}P_2$): C 66.45 (66.15), H 11.10 (11.27). ^{31}P NMR ($CDCl_3$) δ_P/ppm: –33.2 (s). ^{1}H NMR ($CDCl_3$) δ_H/ppm: 1.90–1.65 (m, 8H), 1.63–1.20 (m, 22H). ^{13}C NMR ($CDCl_3$) δ_C/ppm: 31.0 (t, *J*(PC) 10.7 Hz), 29.0 (d, *J*(PC) 13.1 Hz), 28.3 (d, 4.6 Hz), 25.8 (d, *J*(PC) 7.7 Hz), 22.6 (t, PCH$_2$$CH_2CH_2$P, ^2J(PC) 14.6 Hz).

Synthesis of [$PtCl_2(L_5)$] (4a). To a solution of $\mathbf{L_5}$ (0.090 g, 0.416 mmol) in dichloromethane (2 cm^3) was added [$PtCl_2$(cod)] (0.140 g, 0.375 mmol). After stirring the reaction for 12 h, the solvent was removed and the resulting white solid was washed with methanol (10 cm^3) to give the desired product (0.142 g, 0.294 mmol, 79% yield). Elemental analysis, found (calcd for $C_{11}H_{22}Cl_2P_2Pt$): C 27.82 (27.40), H 4.56 (4.60). ^{31}P NMR ($CDCl_3$) δ_P/ppm: 2.8 (s, *J*(PtP) 3323 Hz). ^{1}H NMR ($CDCl_3$) δ_H/ppm: 2.88–2.57 (m, 4H), 2.40–1.59 (m, 18H). ^{13}C NMR ($CDCl_3$) δ_C/ppm: 27.7 (m), 27.3 (m), 23.8 (m), 20.8 (s). EI mass spectrum: *m*/*z* 482 (M^+), 446 (M^+ – Cl), 409 (M^+ – 2Cl).

[$PtCl_2(L_6)$] (4b). Compound **4b** was made in a similar fashion to **4a** from $\mathbf{L_6}$ in 64% yield. Elemental analysis, found (calcd for $C_{13}H_{26}Cl_2P_2Pt$): C 30.42 (30.78), H 5.07 (5.14). ^{31}P NMR ($CDCl_3$) δ_P/ppm: –17.1 (s, *J*(PtP) 3343 Hz). ^{1}H NMR ($CDCl_3$) δ_H/ppm: 2.99–2.81 (m, 4H), 2.05–1.76 (m, 14H), 1.75–1.65 (m, 2H), 1.60–1.38 (m, 6H). ^{13}C NMR ($CDCl_3$) δ_C/ppm: 25.7 (m), 23.2 (m), 22.2 (m), 19.3 (s), 17.8 (m). EI mass spectrum: *m*/*z* 474 (M^+ – Cl), 437 (M^+ – 2Cl).

[$PtCl_2(L_7)$] (4c). Compound **4c** was made in a similar fashion to **4a** from $\mathbf{L_7}$ in 70% yield. Elemental analysis, found (calcd for $C_{15}H_{30}Cl_2P_2Pt$): C 33.43 (33.47), H 5.48 (5.62). ^{31}P NMR ($CDCl_3$) δ_P/ppm: –8.3 (s, *J*(PtP) 3333 Hz). ^{1}H NMR ($CDCl_3$) δ_H/ppm: 2.98–2.78 (m, 4H), 2.14–1.73 (m, 14H), 1.72–1.46 (m, 12H). ^{13}C NMR ($CDCl_3$) δ_C/ppm: 29.3 (s), 28.1 (m), 23.1 (m), 22.1 (m), 18.9 (m). FAB mass spectrum: *m*/*z* 501 (M^+ – Cl-1).

Synthesis of [$Rh_2Cl_2(CO)_2(\mu$–$L_5)_2$] (5a). To a solution of $\mathbf{L_5}$ (0.034 g, 0.157 mmol) in dichloromethane (3 cm^3) was added [RhCl(CO)$_2$]$_2$ (0.030 g, 0.079 mmol) as a solid. After stirring the reaction for 1 h, the solvent was reduced to *ca.* 1 cm^3 and hexane (20 cm^3) was added. The resulting precipitate was filtered off, washed with hexane and dried under reduced pressure to afford the desired product as a light brown powder (0.027 g, 0.071 mmol, 45% yield). Elemental analysis, found (calcd for $C_{24}H_{44}Cl_2O_2P_4Rh_2$): C 37.20 (37.67), H 5.27 (5.80). ^{31}P NMR (CD_2Cl_2) δ_P/ppm: 27.9 (br d, *J*(RhP) 108 Hz), 27.0 (d, *J*(RhP) 113 Hz). ^{1}H NMR (CD_2Cl_2) δ_H/ppm: 2.50–1.30 (br m, 22H, CH_2). ^{13}C NMR (CD_2Cl_2) δ_C/ppm: 32.0–24.4 (m). IR ν_{CO} (CH_2Cl_2): 1968 cm^{-1}. EI mass spectrum: *m*/*z* 708 (M^+ – 2CO).

[$Rh_2Cl_2(CO)_2(\mu$-$L_6)_2$] (5b). Compound **5b** was made in a similar fashion to **5a** from $\mathbf{L_6}$ in 64% yield. Elemental analysis, found (calcd for $C_{28}H_{52}Cl_2O_2P_4Rh_2$): C 41.24 (40.95), H 7.06 (6.38). ^{31}P NMR (CD_2Cl_2) δ_P/ppm: 6.7 (d, *J*(RhP) 117 Hz), 6.0 (d, *J*(RhP) 117 Hz). ^{1}H NMR (CD_2Cl_2) δ_H/ppm: 2.50–1.10 (m, 26H, CH_2). ^{13}C NMR (CD_2Cl_2) δ_C/ppm: 188.7–187.6 (m, *C*O),

Table 8 Crystallographic data

Compound	**4a**·$CHCl_3$	**4b**	**4c**	**5a**	**5c**
Colour, habit	Colourless, block	Colourless, plate	Colourless, block	Yellow, block	Yellow, plate
Size/mm	0.14 × 0.07 × 0.07	0.25 × 0.07 × 0.03	0.14 × 0.10 × 0.06	0.40 × 0.30 × 0.20	0.40 × 0.26 × 0.02
Empirical Formula	$C_{12}H_{23}Cl_5P_2Pt$	$C_{13}H_{26}Cl_2P_2Pt$	$C_{15}H_{30}Cl_2P_2Pt$	$C_{24}H_{44}Cl_2O_2P_4Rh_2$	$C_{32}H_{60}Cl_2O_2P_4Rh_2$
M_r/g mol^{-1}	601.58	510.27	538.32	765.19	877.40
Crystal system	Orthorhombic	Orthorhombic	Monoclinic	Monoclinic	Orthorhombic
Space group	$P2_12_12_1$	*Pbca*	*Pc*	$P2_1/c$	$P2_12_12_1$
a/Å	12.165(2)	12.723(3)	34.324(7)	11.7519(7)	11.0204(18)
b/Å	12.425(3)	11.954(3)	6.3850(13)	11.9472(7)	11.9691(16)
c/Å	12.614(3)	22.007(6)	12.625(3)	22.4102(13)	28.877(3)
β/°	90.00	90.00	92.05(3)	91.1220(10)	90.00
V/Å^3	1906.4(7)	3347.0(15)	2765.1(10)	3145.8(3)	3809.0(9)
Z	4	8	6	4	4
μ/mm^{-1}	8.217	8.878	8.065	1.442	1.202
T/K	100	173	173	173	173
Total reflections	21 202	20 486	28 297	20 348	25 010
Independent reflections	4334	3843	12 421	7198	8754
R_{int}	0.0291	0.0602	0.0296	0.0518	0.0811
Final R_1 ($I > 2\sigma$)	0.0185	0.0292	0.0281	0.0364	0.0444
Final wR_2	0.0468	0.0706	0.0693	0.0795	0.1079
Largest peak, hole (e Å^{-3})	1.06, –0.66	1.65, –1.61	1.76, –1.57	0.65, –0.65	0.62, –0.95
ρ_{calcd}/g cm^{-3}	2.096	2.025	1.940	1.616	1.530
Flack parameter	0.461(5)	—	–0.001(4)	—	–0.01(4)

30.9–20.5 (m). IR ν_{CO} (CH_2Cl_2): 1963 cm^{-1}. EI mass spectrum: *m*/*z* 764 (M^+ – 2CO).

[$Rh_2Cl_2(CO)_2$(μ-L_7)$_2$] (5c). Compound **5c** was made in a similar fashion to **5a** from L_7 in 88% yield. Elemental analysis, found (calcd for $C_{32}H_{60}Cl_2O_2P_4Rh_2$): C 43.75 (43.80), H 6.98 (6.89). ^{31}P NMR (CD_2Cl_2) δ_P/ppm: 18.5 (d, *J*(RhP) 115 Hz), 17.0 (d, *J*(RhP) 115 Hz). ^{1}H NMR (CD_2Cl_2) δ_H/ppm: 2.60–2.29 (m, 2H), 2.13–1.36 (m, 28H). ^{13}C NMR (CD_2Cl_2) δ_C/ppm: 188.8–187.6 (m, *C*O), 32.5–23.9 (m). IR ν_{CO} (CH_2Cl_2): 1960 cm^{-1}. FAB mass spectrum: *m*/*z* 877 (M^+), 720 (M^+ – 2CO).

Hydroformylation catalysis. The phosphine (0.060 mmol) and [$Rh(CO)_2$(acac)] (3.0 mg, 0.012 mmol) were dissolved in toluene (10 cm^3) under nitrogen in a Schlenk tube. The resulting solution was transferred by cannula to a 100 mL autoclave, which had been flushed 3 times with 3 bar CO–H_2 (1 : 1). The autoclave was then pressurized with 2 bar of CO–H_2 (1 : 1) at room temperature. The reaction mixture was then stirred vigorously with a sparging stirrer and heated to 90 °C over a period of 30 min. After this pre-activation of the catalyst, the 1-octene (10 g) was introduced into the autoclave *via* a lock by means of CO–H_2 pressure. The pressure was then immediately raised to 10 bar and maintained at this pressure throughout the catalysis by introduction of further CO–H_2 (1 : 1) *via* a pressure regulator. After running the reactions for 4 h, the autoclave was cooled, vented and emptied. Analysis of the reaction products was carried out by GC.

Crystal structure determinations

X-Ray diffraction experiments of **4b**, **4c**, *syn*-**5a** and *anti*-**5c** were carried out at 173K on a Bruker SMART diffractometer; an experiment on **4a** (as its chloroform solvate) was carried out at 100K on a Bruker SMART APEX diffractometer, all using MoKa radiation (λ = 0.71073 Å). All data collections were performed using a CCD area detector from a single crystal coated in perfluoroalkylether and mounted on a glass fibre. Intensities were integrated[29] from several series of exposures measuring 0.3° in *ω*. Absorption corrections were based on equivalent reflections using SADABS,[30] and structures were refined against all F_o^2 data with hydrogen atoms riding in calculated positions using SHELXTL.[31] Crystal structure and refinement data are given in Table 8. In **4a**·$CHCl_3$ the molecular complex has approximate mirror symmetry, as such that the crystal structure may also be approximately described in the space group *Pnma*, albeit with disorder in the chloroform molecule. The crystal structure refines satisfactorily in $P2_12_12_1$ as an inversion twin (Flack parameter = 0.461(5)). Coupled with the fact that there are a significant number of (albeit weak) reflections present in the diffraction data, which should be systematically absent in *Pnma*, and that the weighted *R*-factor is lower and residual density map is cleaner in the lower symmetry space group, this suggests that $P2_12_12_1$ is the correct choice. In **4c**, the ring containing P(4) has three of the carbon atoms disordered over two positions in proportions 0.66/0.34, and the ring containing P(5) has all of the carbon atoms disordered over two positions (ration 0.57/0.43). The use of restraints on carbon–carbon bond lengths was necessary to ensure convergence of the refinement.

Acknowledgements

We thank BASF and the EPSRC for financial support, Johnson-Matthey for a loan of precious metal compounds and the Leverhulme Trust for a Research Fellowship (to PGP).

References

1 (*a*) P. W. N. M. van Leeuwen, *Homogeneous Catalysis, Understanding the Art*, Kluwer Academic Publishers, Dordrecht, The Netherlands, 2004; (*b*) *Rhodium-Catalysed Hydroformylation*, ed. P. W. N. M. van Leeuwen and C. Claver, Kluwer Academic Publishers, Dordrecht, The Netherlands, 2000.
2 M. Sparta, K. J. Knut and V. R. Jensen, *J. Am. Chem. Soc.*, 2007, **129**, 8487, and references therein.

3 (*a*) E. Billig, A. G. Abatjoglou and D. R. Bryant, Union Carbide, *U.S. Pat.*, 4 599 2061986; (*b*) G. J. H. Buisman, E. J. Vos, P. C. J. Kamer and P. W. N. M. van Leeuwen, *J. Chem. Soc., Dalton Trans.*, 1995, 409; (*c*) A. van Rooy, P. C. J. Kamer, P. W. N. M. van Leeuwen, K. Goubitz, J. Fraanje, N. Veldman and A. Spek, *Organometallics*, 1996, **15**, 5681; (*d*) G. J. H. Buisman, L. A. van der Veen, P. C. J. Kamer and P. W. N. M. van Leeuwen, *Organometallics*, 1997, **16**, 835; (*e*) R. Paciello, L. Siggel, H. Kneuper, N. Walker and M. Röper, *J. Mol. Catal. A: Chem.*, 1999, **143**, 85; (*f*) G. D. Cuny and S. L. Buchwald, *J. Am. Chem. Soc.*, 1993, **115**, 2066; (*g*) G. Erre, S. Enthaler, K. Junge, S. Gladiali and M. Beller, *J. Mol. Catal. A: Chem.*, 2008, **280**, 148, and references therein.

4 (*a*) S. C. van der Slot, P. C. J. Kamer, P. W. N. M. van Leeuwen, J. Fraanje, K. Goubitz, M. Lutz and A. Spek, *Organometallics*, 2000, **19**, 2504; (*b*) M. P. Magee, W. Luo and W. H. Hersh, *Organometallics*, 2002, **21**, 362; (*c*) S. Breedon, D. J. Cole-Hamilton, D. F. Foster, G. J. Schwartz and M. Wills, *Angew. Chem., Int. Ed.*, 2000, **39**, 4106.

5 T. Mackewitz, W. Ahlers, E. Zeller, M. Röper, R. Paciello, K. Knoll, and R. Papp, BASF, *World Pat.*, 200 200 669, 2002.

6 (*a*) B. Breit and E. Fuchs, *Chem. Commun.*, 2004, 694; (*b*) C. Müller and D. Vogt, *Dalton Trans.*, 2007, 5505, and references therein.

7 (*a*) W. Ahlers, BASF, *World Pat.*, 2 001 085 661, 2001; (*b*) W. Ahlers, M. Slany, BASF, *World Pat.*, 2 001 085 662, 2001; (*c*) K. Q. Almeida Lenero, E. Drent, R. van Ginkel, R. I. Pugh, Shell, *World Pat.*, 2 005 058 788, 2005; (*d*) R. A. Baber, M. L. Clarke, K. Heslop, A. C. Marr, A. G. Orpen, P. G. Pringle, A. Ward and D. E. Zambrano-Williams, *Dalton Trans.*, 2005, 1079; (*e*) M. L. Clarke and G. J. Roff, *Chem.–Eur. J.*, 2006, **12**, 7979; (*f*) J. H. Downing, J. Floure, K. Heslop, M. F. Haddow, J. Hopewell, M. Lusi, H. Phetmung, A. G. Orpen, P. G. Pringle, R. I. Pugh and D. Zambrano-Williams, *Organometallics*, 2008, **27**, 3216.

8 (*a*) A. T. Axtell, C. J. Cobley, J. Klosin, G. T. Whitaker, A. Zanotti-Gerosa and K. A. Abboud, *Angew. Chem., Int. Ed.*, 2005, **44**, 5834; (*b*) M. Jackson and I. C. Lennon, *Tetrahedron Lett.*, 2007, **48**, 1831; (*c*) T. P. Clarke, C. R. Landis, S. L. Freed, J. Klosin and K. A. Abboud, *J. Am. Chem. Soc.*, 2005, **127**, 5040; (*d*) A. T. Axtell, J. Klosin and K. A. Abboud, *Organometallics*, 2006, **25**, 5003, and references therein.

9 (*a*) A. G. Orpen and N. G. Connelly, *Chem. Commun.*, 1985, 1310; (*b*) A. G. Orpen and N. G. Connelly, *Organometallics*, 1990, **9**, 1206.

10 J. L. V. Winkle, R. C. Morris, and R. F. Mason, Shell, *Ger. Pat.*, 1 909 620, 1969.

11 (*a*) R. P. J. Bronger, P. C. J. Kamer and P. W. N. M. van Leeuwen, *Organometallics*, 2003, **22**, 5358; (*b*) L. A. van der Veen, P. C. J. Kamer and P. W. N. M. van Leeuwen, *Organometallics*, 1999, **18**, 4765; (*c*) L. A. van der Veen, P. C. J. Kamer and P. W. N. M. van Leeuwen, *Angew. Chem., Int. Ed.*, 1999, **38**, 336; (*d*) T. Hayashi, M. Tanaka and I. Ogata, *J. Mol. Catal.*, 1979, **6**, 1; (*e*) C. F. Hobbs and W. S. Knowles, *J. Org. Chem.*, 1981, **46**, 4422; (*f*) T. J. Devon, G. W. Philips, T. A. Puckette, J. L. Stavinoha and J. J. Vanderbilt, Eastman Kodak, *U.S. Pat.*, 5 332 846, 1994; (*g*) W. A. Hermann, R. B. Manetsberger, G. P. Albanese, H. Bahrmann, and P. Lappe, Ger. Patent, DE 4 333 307 (1994) to Hoechst; (*h*) M. beller, B. Cornils, C. D. Frohning and C. W. Kohlpainter, *J. Mol. Catal. A: Chem.*, 1995, **104**, 17.

12 R. A. Baber, M. F. Haddow, A. J. Middleton, A. G. Orpen, P. G. Pringle, A. Haynes, G. L. Williams and R. Papp, *Organometallics*, 2007, **26**, 713.

13 (*a*) R. Doherty, M. F. Haddow, Z. A. Harrison, A. G. Orpen, P. G. Pringle, A. Turner and R. L. Wingad, *Dalton Trans.*, 2006, 4310; (*b*) M. R. Eberhard, E. Carrington-Smith, E. E. Drent, P. S. Marsh, A. G. Orpen, H. Phetmung and P. G. Pringle, *Adv. Synth. Catal.*, 2005, **347**, 1345; (*c*) M. R. Eberhard, K. M. Heslop, A. G. Orpen and P. G. Pringle, *Organometallics*, 2005, **24**, 335; (*d*) J. H. Downing, V. Gee and P. G. Pringle, *Chem. Commun.*, 1997, 1527; (*e*) D. W. Norman, C. A. Carraz, D. J. Hyett, P. G. Pringle, J. B. Sweeney, A. G. Orpen, H. Phetmung and R. L. Wingad, *J. Am. Chem. Soc.*, 2008, **130**, 6840; (*f*) M. J. Baker, K. N. Harrison, A. G. Orpen, P. G. Pringle and G. S. Shaw, *J. Chem. Soc., Chem. Commun.*, 1991, 803; (*g*) M. J. Baker and P. G. Pringle, *J. Chem. Soc., Chem. Commun.*, 1991, 1292; (*h*) M. J. Baker and P. G. Pringle, *J. Chem. Soc., Chem. Commun.*, 1993, 314; (*i*) C. Claver, E. Fernandez, A. Gillon, K. Heslop, D. J. Hyett, A. Martorell, A. G. Orpen and P. G. Pringle, *J. Chem. Soc., Chem. Commun.*, 2000, 961; (*j*) R. A. Baber, J. G. de Vries, A. G. Orpen, P. G. Pringle and K. von der Luehe, *Dalton Trans.*, 2006, 4821.

14 W. E. Hill, M. Q. Islam, T. S. Webb and C. A. McAuliffe, *Inorg. Chim. Acta*, 1988, **146**, 111.

15 R. W. Alder, C. Ganter, M. Gil, R. Gleiter, C. J. Harris, S. E. Harris, H. Lange, A. G. Orpen and P. N. Taylor, *J. Chem. Soc., Perkin Trans. 1*, 1998, **10**, 1643.

16 (*a*) B. Testa, *Principles of Organic Stereochemistry*, Marcel Dekker, New York, 1979; (*b*) F. A. L. Anet, *Conformational Analysis of Medium-Sized Heterocycles*, ed. R. S. Glass, VCH, New York, 1988; (*c*) G. Favini, *J. Mol. Struct.*, 1983, **93**, 139.

17 (*a*) C. A. Tolman, *Chem. Rev.*, 1977, **77**, 313; (*b*) K. A. Bunten, L. Chen Fernandez and A. J. Poë, *Coord. Chem. Rev.*, 2002, **233–234**, 41, and references therein.

18 B. E. Mann, C. Masters and B. L. Shaw, *J. Chem. Soc. A*, 1971, 1104.

19 (*a*) A. R. Sanger, *J. Chem. Soc., Chem. Commun.*, 1975, 893; (*b*) A. L. Balch and B. Tulyathan, *Inorg. Chem.*, 1977, **16**, 2840.

20 (*a*) A. Roodt, S. Otto and G. Steyl, *Coord. Chem. Rev.*, 2003, **245**, 121; (*b*) M. L. Clarke, G. L. Halliday, A. M. Z. Slawin and J. D. Woollins, *J. Chem. Soc. Dalton Trans.*, 2002, 1093.

21 (*a*) A. R. Sanger, *J. Mol. Catal.*, 1977, **3**, 221; (*b*) M. Tanaka, T. Hayashi and I. Ogata, *Bull. Chem. Soc. Jpn.*, 1977, **50**, 2351; (*c*) C. U. Pittman, Jr. and A. Hirao, *J. Org. Chem.*, 1978, **43**, 640; (*d*) M. Matsumoto and M. Tamura, *J. Mol. Catal.*, 1982, **16**, 195; (*e*) M. Matsumoto and M. Tamura, *J. Mol. Catal.*, 1982, **16**, 209; (*f*) W. Chen, Y. Xu and S. Liao, *J. Mol. Catal. A: Chem.*, 1998, **129**, 153; (*g*) M. Diéguez, M. M. Pereira, A. M. Masdeu-Bultó, C. Claver and J. C. Bayón, *J. Mol. Catal. A: Chem.*, 1999, **143**, 111; (*h*) A. Caiazzo, R. Settambolo, L. Pontorno and R. Lazzaroni, *J. Organomet. Chem.*, 2000, **599**, 298.

22 There is a small decrease in *n*-selectivity in the order $\mathbf{L_5} > \mathbf{L_6} > \mathbf{L_7}$, which, as pointed out by a reviewer, would be the expected trend with increasing donation of the ligand and this is consistent with the thesis of this article.

23 This trend with bite angle is observed for bis equatorially bound ligands; (*a*) P. W. N. M. van Leeuwen, P. C. J. Kamer and J. N. H. Reek, *Pure Appl. Chem.*, 1999, **71**, 1443; (*b*) Z. Freixa and P. W. N. M. van Leeuwen, *Dalton Trans.*, 2003, 1890.

24 (*a*) C. P. Casey, E. L. Paulinsen, E. W. Beuttenmueller, B. R. Proft, L. M. Petrovich, B. A. Matter and D. R. Powell, *J. Am. Chem. Soc.*, 1997, **119**, 11817; (*b*) C. P. Casey, E. L. Paulinsen, E. W. Beuttenmueller, B. R. Proft, B. A. Matter and D. R. Powell, *J. Am. Chem. Soc.*, 1999, **121**, 63; (*c*) T. V. RajanBabu and T. A. Ayers, *Tetrahedron Lett.*, 1994, **35**, 4295.

25 M. L. Clarke, D. Ellis, K. L. Mason, A. G. Orpen, P. G. Pringle, R. L. Wingad, D. A. Zaher and R. T. Baker, *Dalton Trans.*, 2005, 1294.

26 A. B. Pangborn, M. A. Giardello, R. H. Grubbs, R. K. Rosen and F. J. Timmers, *Organometallics*, 1996, **15**, 1518.

27 J. X. McDermott, J. F. White and G. M. Whitesides, *J. Am. Chem. Soc.*, 1976, **98**, 6521.

28 J. A. McCleverty and G. Wilkinson, *Inorg. Synth.*, 1990, **28**, 212.

29 *Bruker SAINT v6.02A (**4b**, **4c**, syn-**5a**, anti-**5c**) or v6.28A (**4a**)*, Siemens Analytical X-ray Instruments Inc., Madison, WI, 1994 or 1998.

30 G. M. Sheldrick, *SADABS v2.03 (**4b**, syn-**5a**), v2.05 (**4a**) or v2.10 (**4c**, anti-**5c**)*, University of Göttingen, Germany.

31 *SHELXTL program system version v5.1*, Bruker Analytical X-ray instruments Inc., Madison, WI, 1998.